Tetrahedron 67 (2011) 8170–8176

Contents lists available at SciVerse ScienceDirect

Tetrahedron

journal homepage: www.elsevier.com/locate/tet

Interaction of chlorobenzene with gelator in methyl-4,6-*O*-(*p*-nitrobenzylidene)-α-D-glucopyranoside gel probed by proton fast field cycling NMR relaxometry

J. Tritt-Goc [a,*], M. Bielejewski [a], R. Luboradzki [b]

[a] Institute of Molecular Physics, Polish Academy of Sciences, ul. M. Smoluchowskiego 17, 60-179 Poznań, Poland
[b] Institute of Physical Chemistry, Polish Academy of Sciences, ul. Kasprzaka 44/52, 01-224 Warsaw, Poland

ARTICLE INFO

Article history:
Received 22 April 2011
Received in revised form 23 July 2011
Accepted 15 August 2011
Available online 22 August 2011

Keywords:
Low-molecular-gel
Solvent–gelator interaction
Spin-lattice relaxation dispersion

ABSTRACT

The solvent–gelator interactions in the gel composed of the low molecular mass gelator methyl-4,6-*O*-benzylidene-α-D-glucopyranoside with chlorobenzene is the subject of the studies. The interaction causes a significant slowing down of the motion of chlorobenzene molecules at the gelator surfaces when compared to bulk chlorobenzene. The motion manifests itself through the low frequency dispersion of the proton spin-lattice relaxation time of chlorobenzene in gel observed below 10^5 Hz. The relaxation time was measured with the Fast Field Cycling relaxometry method in the function of magnetic field strength and temperature. The data were interpreted in terms of two-fraction fast-exchange model.

1. Introduction

A wide variety of low-molecular-mass organic molecules demonstrate the organogelation phenomenon.[1–8] These molecules are named as low-molecular-mass (LMOGs) or low-molecular-weight (LMWGs) gelators. The resulting gels (organogels in cases where the solvent is an organic compound or hydrogel when it is water) are formed by the self-aggregation of gelator molecules, leading to the formation of three-dimensional matrices of networks of nanofibres that immobilize the solvent. Gelator molecules in the fibers are self-assembled through non-covalent interactions, such as electrostatic, dipole–dipole, hydrogen-bonding (H-bonding), the π–π stacking, and van der Waals interactions and therefore the gels are classified as physical gels. The gels retain the solid-like rheological properties despite being predominantly liquid in composition. Usually 99% of the gel by weight is liquid and only 1% is gelator. The molecules' arrangement within the nanofibres, regardless of their random entanglement, displays significant order. Unidirectional intermolecular structure is usually observed.

The gels made by LMOGs represent soft materials that are receiving considerably increasing attention[9] because of their current and possible numerous applications but also because detailed knowledge about the molecular assemblies is necessary for sensible design of these materials.[1,7,10–12] The extensive studies of the organogels have improved the understanding of the self-organization of gelator molecules into a three-dimensional network structure and the gelation phenomenon, but some questions remain. It is still a challenge to predict whether a molecule can act as a gelator. The molecular interactions governing gelation, i.e., the gelator–gelator interactions, are well known and recognized typically by nuclear magnetic resonance (NMR) or Fourier transform infrared (FTIR) spectroscopy.[13–15] On the other hand the solvent–gelator interactions remain ambiguous. There are many examples in the literature showing the dependence of the thermal stability and of the gel morphology upon the gelated solvent (polarity, concentration, and pH condition).[1,15–23] Different approaches are used to quantify solvent effects employing solvent parameters, such as dielectric constant, Hildebrand's solvent polar solubility, Reichardt's $E_T(30)$ parameter scale, Hansen hydrogen solubility index or Kamlet–Taft parameters.[15,18,24–27] However, the question about the interaction of the solvent molecules with LMOGs aggregates in the gel is still open.

We reported in a previous paper experimental evidence of solvent–gelator interactions in a gel composed of sugar based 1,2-*O*-(1-ethylpropylidene)-α-D-glucofuranose with toluene obtained with the ^{1}H Fast Field Cycling (FFC) relaxometry method.[28–30] The toluene molecules in interaction with the surface of an organogel are responsible for the observed dispersion of the relaxation rate T_1^{-1} of toluene in the frequency range 10^4–10^6 Hz. Recently, comparable dispersion of toluene was observed in an organogel built with modified amino-acids.[31] These two cases are believed to be so far (to the best of our knowledge) the first experimental verification of the interaction of solvent molecules with the fibers of organogels.

* Corresponding author. Tel.: +48 061 8695 226; e-mail address: jtg@ifmpan.poznan.pl (J. Tritt-Goc).

0040-4020/$ – see front matter © 2011 Published by Elsevier Ltd.
doi:10.1016/j.tet.2011.08.040

The FFC method with the commercially available relaxometer Stelar FFC2000 allows the study of the molecular dynamics in the frequency range from 10 kHz to 40 MHz and therefore is very suitable for the study of the dynamics of a liquid confined in the pore structure.[30] The gels made by LMOGs consist of a three-dimensional fibrillar network, which entraps a huge amount of solvent molecules in the spaces (pores) within the network and can be treated like a porous material. Liquid confined to pores shows different physical properties than in bulk. Besides the shifts of melting and freezing temperatures, an orientational ordering of the liquid molecules at the pore surface, anomalous diffusion, and enhancement of correlation times by 6–8 orders of magnitude, as compared to bulk liquid, is observed. The significant slowing down of the correlation time of the solvent molecules confined in pores can be due to the solvent–gelator interactions and/or confinement effect.[30] The former effect is predominantly responsible for the low magnetic field dispersion of the solvent relaxation rate, if such is observed in the studied gels.[28–31] The latter effect can be excluded in the case of gels made by LMOGs due to the large pores within the fibrillar matrix of gels.

In an attempt to better understand the solvent–gelator interactions, this paper reports the investigation of a gel composed of methyl-4,6-*O*-(*p*-nitrobenzylidene)-α-D-glucopyranoside and chlorobenzene. This compound is unique not only in the family of sugar-based gelators but also in the large group of LMOGs because it has the ability to gelate various organic solvents and water.[19] Such 'bifunctional' gelators are limited in the literature.[8] It can also serve as an acceptor group in novel donor–acceptor, sugar-based gelators, which exhibit a charge transfer interaction.[32,33] The crystal structure for the studied gelator has not been examined but it is reasonable to assume, that is, very similar to the methyl-4,6-*O*-benzylidene-α-D-glucopyranoside.[34,35] The studied gelator differs only by the nitro group attached to the benzylidene in the *para*-position. In the crystal state, the unsubstituted gelator forms one-dimensional zigzag chains in which molecules are connected by two intermolecular hydrogen bonds using the hydroxyl group 2-OH and 3-OH. Such unidirectional formation of the hydrogen bonds network is a precondition for the molecules to be a good gelator.[1] It was shown that only the introduction of *p*-nitro-substituent in *para*-position increases the ability for self-aggregation of methyl-4,6-*O*-benzylidene-monosaccharides.[19] In non polar solvents the hydrogen-bond interactions are the driving forces for self-assembly of this type of gelators, whereas in water other aggregation modes, such as dipole–dipole, hydrophobic or the π–π stacking interactions dominate the self-assembly.[8,19]

The thermal properties, the microstructure of methyl-4,6-*O*-(*p*-nitrobenzylidene)-α-D-glucopyranoside hydrogel, and the molecular dynamics of water in the gel network structure were the subject of previous paper.[36]

In the present contribution we focused on the proton spin-lattice relaxation measurements (T_1) of chlorobenzene in the methyl-4,6-*O*-(*p*-nitrobenzylidene)-α-D-glucopyranoside gel measured as the function of the temperature and magnetic field. The aim of our study was to detect the chlorobenzene–gelator interactions through the spin-lattice relaxation dispersion measurements using the FFC method.

2. Theoretical background of proton NMR relaxation

The predominant contribution to the spin-lattice relaxation mechanism for protons (^{1}H), nuclei with spin ½, is based on dipole–dipole couplings, which can be intramolecular and intermolecular in nature. The intramolecular interactions involve protons belonging to the same molecule. Their time dependence is due to the fluctuation of the orientation of the dipole–dipole axes caused by the rotational diffusion of the molecules. The intermolecular dipole–dipole coupling occurs between protons belonging to different molecules and in addition the fluctuation of the interproton distance has to be taken into account. The fluctuation occurs through the translational motions of the whole molecules over distances larger than the dimensions of the molecule. With the assumption of stochastic independence of the two types of fluctuating dipole–dipole couplings both additively contribute to the spin-lattice relaxation $T_1^{-1} = T_{1\text{intra}}^{-1} + T_{1\text{inter}}^{-1}$. Usually, the intramolecular contribution dominates the relaxation due to the short range nature of dipole–dipole interactions. For intramolecular interactions of equivalent spins ½, like protons, the expression of the spin-lattice relaxation rate is given by Blombergen, Purcell, and Pound (BPP)[37]

$$\frac{1}{T_1} = C_{\text{DD}}[J_1(\omega_0) + 4J_2(2\omega_0)] \tag{1}$$

where $\omega_0=\gamma B_0$ is the resonance angular frequency, B_0 is the external magnetic flux density, C_{DD} is the dipole–dipole constant, and J is the spectral density function. If the correlation function, which describes the correlation time of the fluctuating spin is defined by

$$G(t) = \exp\{-|t|/\tau\} \tag{2}$$

then the spectral density functions J in Eq. 1, being the Fourier transform of the correlation function, takes the form:

$$J_1(\omega_0) = J_2(\omega_0) = \frac{2\tau_c}{1+\omega_0\tau_c^2} \tag{3}$$

Finally, the full expression for the spin-lattice relaxation rates is written as:

$$\frac{1}{T_1} = C_{\text{DD}}\left(\frac{\tau_c}{1+\omega_0^2\tau_c^2} + \frac{4\tau_c}{1+4\omega_0^2\tau_c^2}\right) \tag{4}$$

The temperature dependence of the correlation time τ_c responsible for the magnetic relaxation in Eq. 4 can be described by the Arrhenius equation:

$$\tau_c = \tau_0 \exp(E_a/RT) \tag{5}$$

where: R-gas constant, T-absolute temperature, τ_0-constant, E_a-energy barrier for molecule reorientation; or by the Debye–Stokes–Einstein equation, which relates the correlation time τ_c to the macroscopic viscosity η of the solvent:

$$\tau_c = \frac{4\pi r^3 \eta}{3k_B T} \tag{6}$$

In Eq. 6 k_B is the Boltzmann's constant, T is the absolute temperature, and r is the hydrodynamic radius of the molecule.

For the solvent containing molecular oxygen (i.e., non degassed solvent) the paramagnetic contribution from molecular oxygen to the proton spin-lattice relaxation has to be taken into account. The simplified equation for the relaxation can take the following form:[38]

$$\frac{1}{T_1} = A\left(\frac{\tau_s}{1+\omega_s^2\tau_s^2}\right) + B \tag{7}$$

where A is a constant, ω_s is the electron Larmor frequency, and τ_s is the correlation time for the electron–nuclear coupling. The first term in the Eq. 7 includes the dispersion from the electron Larmor frequency, whereas constant B is the contribution connected with the nuclear Larmor frequency. The constant A includes the magnetogyric ratios of the proton and the electron, the oxygen concentration, the intermoment distance, and the usual physical constants.

There are different models applied to the interpretation of the nuclei spin-lattice frequency dispersion data of liquid in pores. Among them magnetic cross-relaxation[39,40] two-phase fast-exchange model,[41] and more complicated models like the bulk-mediated surface diffusion (BMSD)[30,42] and reorientation mediated by translational displacements (RMTD).[30,42] The combination of two latter models leads to the efficient spin-lattice relaxation mechanism only in the strong absorption case where the polar solvent interacts with a strong polar surface.[30] This is not the case of the studied gel. The methyl-4,6-*O*-(*p*-nitrobenzylidene)-α-D-glucopyranoside gelator, like other carbohydrates, creates a polar surface but chlorobenzene is a relatively weak polar solvent. Taking into account dielectric constant as a rough measure of a solvent's polarity, chlorobenzene can be generally considered to be non polar when compared to a strongly polar solvent like water (ε=5.6 and ε=80 for chlorobenzene and water, respectively).

The magnetic cross-relaxation mechanism was successfully used in the interpretation of the proton relaxation dispersion data of water in gel systems or proteins[39,40] but does not apply for chlorobenzene confined in the methyl-4,6-*O*-(*p*-nitrobenzylidene)-α-D-glucopyranoside gel. There are two major contributions to cross-relaxation: the direct dipole–dipole coupling between diffusing solvent protons and the protons of solid gel matrix, and the chemical exchange of unstable protons of the gel matrix (i.e., hydroxyl groups) with solvent protons. Chlorobenzene does not have exchangeable protons hence the chemical exchange phenomenon cannot happen. As discussed in the literature, the contribution to the solvent proton–gelator proton interactions modulated by translation diffusion of solvent molecules is very small because the effective diffusion coefficient of the solvent molecules at the surface of pores is not very different from that in the bulk.[30] Consequently, the correlation time for coupling is short and the relaxation effectiveness low.

The two-phase fast-exchange model[41] is the one used in the interpretation of the measured relaxation dispersion data of chlorobenzene in methyl-4,6-*O*-(*p*-nitrobenzylidene)-α-D-glucopyranoside gel. This model assumes two states or fractions of solvent molecules: one, which is next to the surface of the gelator aggregates (or at the pore surface) called the motionally altered fraction and the other 'inside' the pores that behaves like bulk solvent (no altered fraction). In this model the observed relaxation rate is a linear combination of the bulk and surface contributions[43]

$$\frac{1}{T_{1\mathrm{obs}}} = \frac{f}{T_{1\mathrm{b}}} + \frac{1-f}{T_{1\mathrm{s}}} \tag{8}$$

where f is the fraction of the solvent in the pores, which behaves as in bulk and $1-f$ is the fraction of the solvent at the pore surface, respectively. $T_{1\mathrm{b}}$ is the spin-lattice relaxation time for the bulk solvent and $T_{1\mathrm{s}}$ the relaxation time of solvent protons at the pores' surface. The exchange rate between surface-affected and bulk molecules is much faster than the relaxation rate in each of the phases. Experimentally, the two-fraction fast-exchange model is justified by a single value of the spin-lattice relaxation time.

3. Results and discussion

3.1. The gel–sol (T_{gel}) phase transition temperature

The gelation process of methyl-4,6-*O*-(*p*-nitrobenzylidene)-α-D-glucopyranoside with chlorobenzene as a solvent has been studied for different gelator concentrations. The T_{gel} phase transition temperature was determined by the visual inspection of the samples in air-bath method. The temperature was defined as the one at which the gel starts to flow. The influence of the gelator concentration on the gel-to-sol phase transition temperature is shown in Fig. 1 as a plot of T_{gel} versus gelator concentration. An exponential increase of gel–sol temperature with gelator concentration is observed. The measured T_{gel} value, for concentration of 2% [g/mL] of the gelator used to form the gel with chlorobenzene, which is the subject of the study, is equal to 334 K. The knowledge of the gel–sol (T_{gel}) phase transition temperature was required to analyze the temperature dependence measurements of the spin-lattice relaxation dispersion of the solvent in the gel.

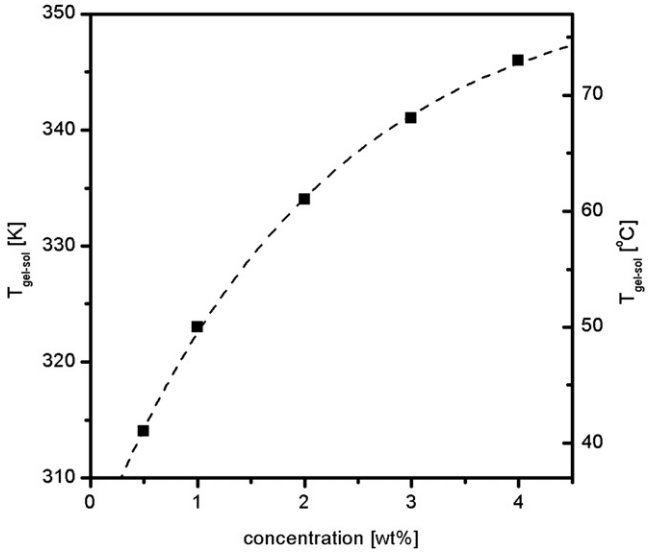

Fig. 1. The dependence of gel-to-sol phase transition, T_{gel}, on the methyl-4,6-*O*-(*p*-nitrobenzylidene)-α-D-glucopyranoside gelator concentration in chlorobenzene gel.

3.2. Proton spin-lattice relaxation dispersion for bulk chlorobenzene

The magnetic field dependence of proton spin-lattice relaxation rates T_1^{-1} (Nuclear Magnetic Resonance Dispersion profile) of chlorobenzene in gel is used to determine the solvent–gelator interactions. The results of our previous studies revealed that such an interaction manifests itself by solvent relaxation dispersion in the gel system in a low frequency range of 10^4–10^6 Hz.[28] To be sure that the dispersion is solely due to the interaction between the solvent and the pore surface of the gelator aggregates and not somehow connected with the solvent itself, we first performed the measurements for bulk chlorobenzene.

Proton spin-lattice relaxation rates for bulk chlorobenzene at 273 K are shown in Fig. 2 as a function of the magnetic field strength but reported as the proton Larmor frequency. In the absence of oxygen, for degassed solvent (open squares), no dependence of chlorobenzene proton spin-lattice relaxation rate T_1^{-1} was observed over the frequency range studied. The reason is that only the proton dipole–dipole interactions modulated by rotational and translational motions of solvent molecules contribute to the T_1^{-1} and consequently, the dispersion occurs in the higher frequency range because the correlation time (the inverse of the frequency at which the maximum dispersion occurs) is in the range of 10^{-12} s or higher. The relaxation rate value is constant over the measured frequency range and equal 0.09 s^{-1}.

For non degassed chlorobenzene, filled circles on Fig. 2, in comparison to the degassed solvent, an increase of the relaxation rate T_1^{-1} (decrease of T_1) to 0.40 s^{-1} and a shift of the frequency at which the maximum dispersion occurs toward the lower value were observed. These two effects are identified with the paramagnetic contribution from the molecular oxygen in the non degassed sample. Therefore, the electron–nuclear coupling,[38] beside nuclei dipole–dipole contribution, has to be considered to fully

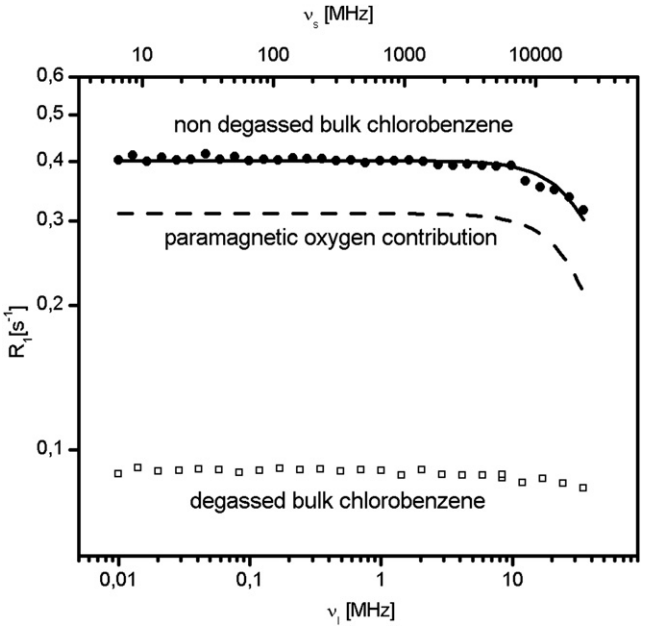

Fig. 2. Proton spin-lattice relaxation rates of degassed (open squares) and non degassed (filled circles) bulk chlorobenzene at 273 K measured as a function of the magnetic field strength reported as the proton Larmor frequency (bottom) and electron Larmor frequency (top). The solid line through the filled circles represents the best fit of Eq. 7 to the experimental points. The dashed line represents the paramagnetic contribution.

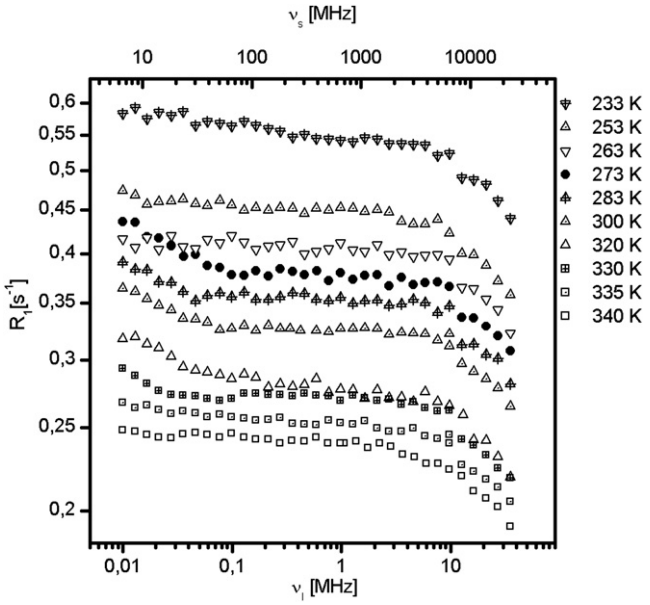

Fig. 3. Magnetic-field dependences of proton spin-lattice relaxation rates of chlorobenzene confined in the pores of studied gel at different temperatures. The dispersion curve at 273 K (filled circles) was the subject of our analysis as discussed in the text.

analyze the proton spin-lattice relaxation dispersion for chlorobenzene. This former contribution is expected to be dominated by the relative translational motion of the oxygen molecules and chlorobenzene protons. Eq. 7 was used to fit the T_1^{-1} data for oxygenated solvent presented in Fig. 2. The constant B in Eq. 7 was taken to be equal to the value of the measured spin-lattice relaxation rate for degassed chlorobenzene (0.09 s^{-1}). The solid line through the filled circles shown in Fig. 2 presents the best fit with the fitting parameters τ_s and A, correspondingly equal 4.70×10^{-12} s and 6.60×10^{10}. The dashed line shows the paramagnetic contribution from the molecular oxygen to the relaxation rate data. The electron spin relaxation parameters obtained for oxygenated chlorobenzene compared well with those obtained for other oxygenated solution of organic solvents.[28,38]

The results presented in Fig. 2 for bulk chlorobenzene (non degassed as well as for the degassed sample) clearly demonstrate that no dispersion of the relaxation rate is observed in the low frequency range 10^4–10^6 Hz.

3.3. Proton spin-lattice relaxation dispersion for chlorobenzene in gel

Fig. 3 shows the temperature dependence of nuclear magnetic dispersion profiles of chlorobenzene in methyl-4,6-*O*-(*p*-nitrobenzylidene)-α-D-glucopyranoside gel. It is clearly seen that in contrast to bulk chlorobenzene, in the temperature from 273 K to 330 K, the NMRD profile of this solvent in the gel exhibits an extra dispersion at frequencies below 10^5 Hz, indicating the presence of a molecular dynamic process with characteristic frequency in the kHz range not found in the bulk chlorobenzene. Therefore, we assumed that the dispersion observed in the frequency range 10^4–10^5 Hz is due to the interaction between the chlorobenzene and the surface of gelator aggregates, which formed the solid fibrillar networks in the gel. This interaction is fundamental to understanding the observed magnetic field dependence of the spin-lattice relaxation rate.

Different models can be used to explain this phenomenon but as considered earlier the two-phase fast-exchange model[41] is the one most suitable to the interpretation of the measured relaxation dispersion data of chlorobenzene in methyl-4,6-*O*-(*p*-nitrobenzylidene)-α-D-glucopyranoside gel. This model is further favored by the fact that the observed relaxation decays were monoexponential and could be well fitted by a single value of value of the T_1 over the full temperature range. Moreover, the type of the temperature dependence of the relaxation rate of chlorobenzene confined in the gel (Fig. 3) provides the evidence that the exchange process of the chlorobenzene molecules in the vicinity of the surface of the gelator with that 'inside' the pores-bulk chlorobenzene takes place by translational diffusion. The relaxation rate increases with decreasing temperature and this is qualitatively consistent with a diffusion-induced relaxation process.

In Fig. 3 the magnitude of the low frequency dispersion increases gradually with decreasing temperature with its highest value found at 273 K. Therefore, the proton spin-lattice relaxation rate of chlorobenzene in gel at this temperature was a subject of our analysis. These experimental data are presented alone in Fig. 4 together with the calculated lines obtained on the base of the two-fraction fast-exchange model.

In the studied case the observed relaxation rate is not only a linear combination of the bulk and surface relaxations as given by Eq. 8 but also the paramagnetic contribution from molecular oxygen (Eq. 7) has to be taken into account. The final equation modified for our purpose takes the following form:

$$\frac{1}{T_{1\mathrm{obs}}} = \frac{f}{T_{1\mathrm{b}}} + \frac{1-f}{T_{1\mathrm{s}}} + A\left(\frac{\tau_s}{1+\omega_s^2\tau_s^2}\right) \tag{9}$$

In Eq. 9 the first term is connected with the fraction f of chlorobenzene in the pores, which behaves as in bulk, the second one describes the contribution from the fraction $1-f$ of the chlorobenzene at the surface of the aggregates (motionally altered fraction of chlorobenzene) and the third term contains the contribution from the molecular oxygen in non degassed solvent. The $T_{1\mathrm{b}}$ and $T_{1\mathrm{s}}$ are the spin-lattice relaxation times for the bulk chlorobenzene and chlorobenzene protons at the gelator aggregates, respectively.

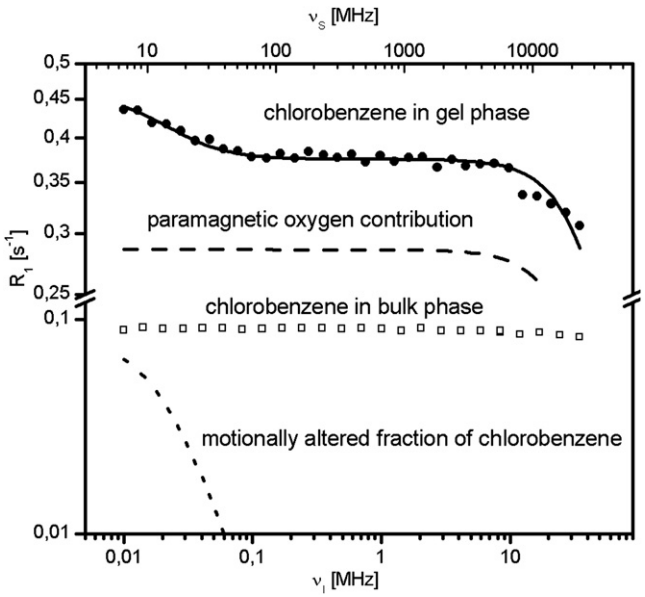

Fig. 4. Proton spin-lattice relaxation rates of chlorobenzene in methyl-4,6-*O*-(*p*-nitrobenzylidene)-α-D-glucopyranoside gel measured as a function of the magnetic field strength reported as the proton Larmor frequency (bottom) and electron Larmor frequency (top) at 273 K. The solid line through the filled circles is the best fit of Eq. 7 to the experimental points calculated as a sum of the contributions from paramagnetic oxygen contribution (long dashed line), bulk chlorobenzene (open squares), and chlorobenzene at pore surface (short dashed line).

Because the T_{1b} is constant over the whole experimentally accessible frequency range the observed dispersion in the frequency range 10^4–10^5 Hz shown in Fig. 4 is entirely determined by the fraction of the chlorobenzene molecules at the gelator surface.

Powel and co-workers[44,45] carefully analyzed the temperature dependence of proton spin-lattice relaxation time for benzene and its derivatives including chlorobenzene. They have shown that the dipole–dipole interactions between ring protons modulated by its reorientations are a main relaxation mechanism. The activation energy for reorientation of the chlorobenzene ring estimated from their data is equal E_{ab}=9.90 kJ mol^{-1}. We assumed that the same relaxation mechanism is true for chlorobenzene in the gel phase. Therefore, T_{1s}^{-1} in Eq. 9 was described by the formula expressed by Eq. 4. In the first approach the correlation time was described by the Arrhenius—Eq. 5.

Eq. 9 after inserting Eqs. 4 and 5 was used to fit the experimental data shown in Fig. 4. The solid line through the filled circles is the best fit of this equation to the experimental data. Two dashed lines reflected the contribution from the molecular oxygen and the protons from the ring of motionally altered fraction of chlorobenzene in gel, respectively. In Fig. 4 the no altered fraction of chlorobenzene, which behaves as bulk is also shown (open squares), whose contribution to the measured relaxation is given by a constant value. As can be seen the bulk and pore surface contributions depend on the field strength. The surface contribution is dominant at lowest filed strength and is responsible for the observed dispersion. The fitted values for the activation energy and τ_{0s} constant of the fraction of chlorobenzene at the pore surface are: E_{as}=11.79 kJ mol^{-1} and τ_{0s}=2.43×10^{-8} s^{-1} (corresponds at 273 K to the value of τ_{cs}=1.90×10^{-6} s), respectively. These values differ from those for bulk chlorobenzene and indicate that the motion of the chlorobenzene ring is significantly restricted at the surface.

Liquid confined to pores shows different physical properties than in bulk.[30] Interactions with the surface can result in the enhancement of correlation times by 6–8 orders of magnitude as compared to bulk solvent. For example, water confined in Bioran B30 is characterized by a correlation time of up to 10^{-4} s, whereas the rotational correlation time in bulk water is in the order of 10^{-12} s at room temperature.[46] The enhancement of the correlation time was found also for toluene confined in the 1,2-*O*-(1-ethylpropylidene)-α-D-glucofuranose gel.[28] The long correlation time for the chlorobenzene ring protons is another example of this phenomenon. The chlorobenzene in gel is confined in the three-dimensional network forms by the methyl-4,6-*O*-(*p*-nitrobenzylidene)-α-D-glucopyranoside gelator molecules. We claimed that the long correlation time of chlorobenzene ring results from the solvent–gelator interaction. Thanks to this interaction the chlorobenzene molecules tend to adopt a preferential orientation with respect to the surface.

The question arises about the origin of the orientation of chlorobenzene molecules at the pore surface. We assume that it comes from the interaction between the electric dipolar moment of the chlorobenzene molecules and polar surface composed of methyl-4,6-*O*-(*p*-nitrobenzylidene)-α-D-glucopyranoside aggregates.

The fitting value of the fraction of motionally altered chlorobenzene responsible for the observed dispersion of the spin-lattice relaxation is 0.03. Such a small population of molecules with orientational dynamics that are retarded at the pore surface explains why the observed dispersion is so weak. It also proves the sensitivity of the field-cycling technique in the study of the solvent–surface interaction in gel systems.

On the basis of our data we can estimate how many of the solvent molecules are immobilized per gelator molecule. The molar mass of the chlorobenzene is equal to 112.560 [g/mol], the mass of the solvent used for sample preparation is equal to 0.199 [g] thus it is equal to 1.768×10^{-3} mol and that gives 1.065×10^{21} molecules of chlorobenzene. The molar mass of the gelator is equal to 321.240 [g/mol], the mass of the gelator used in sample preparation is equal to 0.004 [g] and that gives 1.265×10^{-5} mol equal to 7.611×10^{18} molecules. The fraction of motionally altered solvent is 3%, which gives 3.194×10^{19} molecules of chlorobenzene. If we assume that all of the gelator molecules are on the surface, then the mean number of solvent molecules per gelator molecules is equal to about 4. The solvent molecules at the gelator surface are in fast exchange with the solvent molecules in the bulk phase but at any particular time, one molecule of the gelator interacts with four molecules of the solvent. However, if we take into account all solvent molecules in the gel structure, that is, the motionally altered fraction as well as the bulk fraction, then one gelator molecule immobilizes about 140 molecules of chlorobenzene.

The fitting parameters τ_s and A, describing the contribution from the molecular oxygen in non degassed solvent in the gel system were equal to that obtained for the bulk solvent (4.73×10^{-12} s and 6.57×10^{10}, respectively).

The experimental data in Fig. 4 were also analyzed assuming Debye–Stokes–Einstein formulas for correlation time and thus relating the microscopic relaxation time of a solvent in gel with its macroscopic viscosity. The fit of Eq. 9 after inserting Eqs. 4 and 6 gave the same result (not shown in Fig. 4) as when analyzing the data with the assumption that the correlation time fulfills the Arrhenius equation. The interesting result concerns the value of the fitting viscosity parameter. The viscosity change at the pore surfaces as compared to the bulk and is equal 19.67 Pa s.

The low frequency dispersion of the proton spin relaxation for chlorobenzene occurs in the temperature range from 273 to 330 K but disappears above 330 K and below 273 K (Fig. 4). The T_{gel} value, for studied gel was measured to be 334 K (Fig. 1). Therefore, above 330 K the transition from gel to liquid phase takes place and in the liquid phase no dispersion is observed. This fact supports our conclusion that the dispersion is due to the solvent–gelator matrix interactions.

What is unclear is the behavior of the dispersion below 273 K.

We performed separate experiments on the gel with cooling the sample to 273 K, next lowering the temperature to 263 K and once again heating the gel to 273 K. At each temperature the relaxation measurements in the studied frequency range were performed. The results are presented in Fig. 5 and clearly show that the dispersion visible at 273 K (filled small circles) disappears with the cooling of the gel to 263 K (open triangles) and reappears when increasing the temperature to 273 K (open circles). This process is reversible and had been repeated several times. The observed phenomenon can be connected with the mean residence time of solvent molecules on the pore surface. Below 263 K the mean residence time of the solvent molecules on the pore surface can become too long and therefore the relaxation by a surface becomes inefficient.

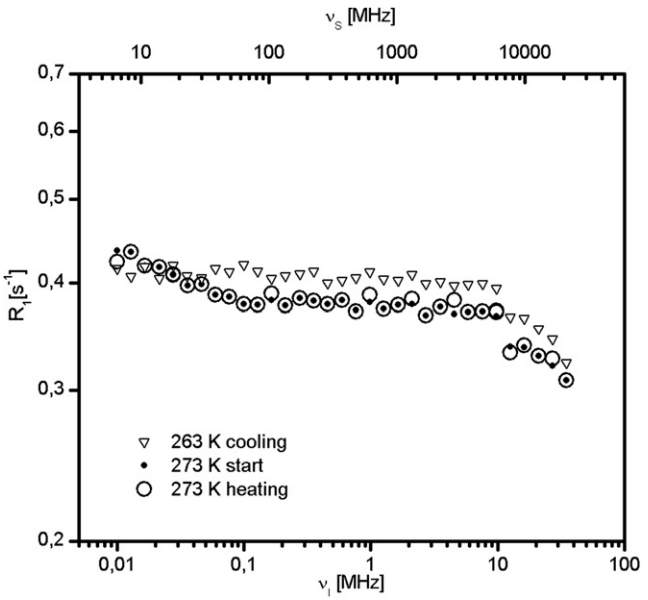

Fig. 5. The behavior of the proton spin-lattice relaxation rates of chlorobenzene in methyl-4,6-*O*-(*p*-nitrobenzylidene)-α-D-glucopyranoside gel measured as a function of the magnetic field strength reported as the proton and electron frequency during cooling and heating the gel sample in the temperature cycle 273 K–263 K–273 K.

3.4. Aging effect

The relaxation measurements were performed on a newly prepared gel. An interesting feature was observed on the 6 month aged sample. The sample was unchanged by visual inspection. It also 'passed' the inverted tube test. On this gel we performed the spin-lattice relaxation measurement in the same temperature range as for a freshly prepared gel. The values of the relaxation at particular temperature were the same for both samples. However, on the aged sample the dispersion at low frequency was not observed at any studied temperature. There are reports in the literature that due to aging, viscoelastic properties and structure changes of colloidal glasses and gels are observed.[47–50] Our finding indicates that also solvent–gelator interactions evolve with time.

4. Conclusion

The ^{1}H field-cycling nuclear magnetic resonance relaxometry was used to study the spin-lattice relaxtion time of chlorobenzene confined in the methyl-4,6-*O*-(*p*-nitrobenzylidene)-α-D-glucopyranoside gel as a function of the magnetic field strength and temperature. The results were interpreted in terms of a two-fraction fast-exchange model that assumes that exchange between the surface and bulk-like populations occurs on a time scale, that is, faster than that of surface and in the bulk, and therefore is directly observable in the NMR signal. Based on this model, by fitting of Eq. 9 to the experimental T_{1obs}^{-1} versus the magnetic field strength (or proton Larmor frequency) the separation into two contributions was accomplished.

The results clearly evidence that the solvent molecules at the gelator surface are characterized by the correlation time much slower when compared to the bulk liquid and are responsible for the magnetic field dispersion of the solvent proton relaxation rate observed below 10^5 Hz. The slowing down of the motion of chlorobenzene at the gelator surface is a consequence of the solvent–gelator interaction. The bulk-like and surface chlorobenzene populations in the gel were estimated and have been shown that they differ considerably (0.97 and 0.03, respectively).

This work provides further evidence of solvent–gelator interactions in the LMOG gels and proves that the FFC method is best suitable for their study, mostly due to its sensitivity to the type of molecular dynamics involved. It is able to reveal an amount of solvent molecules interacting with the gelator fibers as low as 0.02 as shown in our previous studies concerning gel composed of toluene and LMOGs 1,2-*O*-(1-ethylpropylidene)-α-D-glucofuranose where the solvent–gelator interactions were detected for the first time.[28]

5. Experimental section

5.1. Materials

LMOG methyl-4,6-*O*-(*p*-nitrobenzylidene)-α-D-glucopyranoside was synthesized according to a method described elsewhere.[19] The presence of the nitro group in the *p*-position induces a strong ability to gelate different solvents among them chlorobenzene. This solvent was obtained commercially from the Aldrich Chemical Co. and was used as received.

5.2. Procedure for making gel

A concentration of 2% [g/mL] of the gelator was chosen to form the gel with chlorobenzene. The gel was prepared by mixing the required amount of the methyl-4,6-*O*-(*p*-nitrobenzylidene)-α-D-glucopyranoside and chlorobenzene in a closed capped tube and heating the mixture until the complete dissolution of the solid. Cooling the solution below the characteristic gelation temperature brings out the transition to the gel phase. As a result a thermoreversible, optically clear and transparent gel is obtained. Methyl-4,6-*O*-(*p*-nitrobenzylidene)-α-D-glucopyranoside based gel has to be prepared with non degassed chlorobenzene. Like in other physical gels, also in the studied one there are different physical factors affecting the gel preparation and its properties. The pressure is one of the key factors and if it is too low the methyl-4,6-*O*-(*p*-nitrobenzylidene)-α-D-glucopyranoside chlorobenzene gel will not form.

5.3. Procedure for measuring gelation temperature

Thermal stabilities of the gel were analyzed by the air-bath method and visual inspection of the samples. The air-bath method involves inserting a sample into a stream of continuous nitrogen gas flow, whose temperature changes are precisely controlled. For this purpose, we used a slightly modified NMR probe head. The opaque radio-frequency coil was replaced by a transparent glass tube, and thus, a visual inspection of the sample was possible. The temperature of the gel–sol (T_{gel}) transition was determined upon heating the sample to the temperature at which the system starts to flow and was measured with an accuracy of ±0.5 K.

5.4. Procedure for measuring the relaxation time

Proton spin-lattice relaxation measurements of bulk chlorobenzene and chlorobenzene in the gel, in the function of magnetic field B_0, were performed on field-cycling relaxometer (STELAR Company) covering proton frequencies from 10 kHz to 40 MHz. The spectrometer operates by switching current in specially designed solenoid from a polarizing field (B_{POL}) with a ^{1}H Larmor frequency of 24 MHz to a field of interest (B_{RELAX}) for a variable relaxation period (τ) after which the field is switched to a ^{1}H Larmor frequency of 16 MHz (B_{ACQ}) where the magnetization is detected by a $\tau-\pi/2$ pulse sequence. The switching time was 3 ms. Free Induction Decay signal was measured as a function of the delay time τ at the field of interest B_{RELAX}. The relaxation time T_1 was calculated from the recovery or decay of the magnetization. A single exponential relaxation was observed in all cases. The measurements were carried out in the temperature range from 233 K to 340 K. The temperature was controlled by heating flowing air or evaporating nitrogen. The measured nuclear magnetic resonance (NMR) signal in the gel comes only from the chlorobenzene protons. The contribution of the gelator aggregates protons, which form the rigid matrix in the gel phase with strongly restricted motion, are undetectable under our NMR measuring conditions.

The relaxation data for bulk degassed and non degassed chlorobenzene samples were performed for comparison and to check the possible influence of the molecular oxygen on the relaxation dispersion.

Acknowledgements

This work has been supported by funds from the National Centre for Science as research project N N202 1961 40.

References and notes

1. Weiss, R. G.; Terech, P. *Molecular Gels, Materials with Self-Assembled Fibrillar Network*; Springer: Dordrecht, The Netherlands, 2006.
2. George, M.; Weiss, R. G. *Acc. Chem. Res.* **2006**, *39*, 489–497.
3. Estroff, L. A.; Hamilton, D. *Chem. Rev.* **2004**, *104*, 1201–1218.
4. Terech, P.; Weiss, R. G. *Chem. Rev.* **1997**, *97*, 3133–3159.
5. Llusar, M.; Sanchez, C. *Chem. Mater.* **2008**, *20*, 782–820.
6. Samai, S.; Dey, J.; Biradha, K. *Soft Matter* **2011**, *7*, 2121–2126.
7. Piepenbrock, M. O. M.; Lloyd, G. O.; Clarke, N.; Steed, J. W. *Chem. Rev.* **2010**, *110*, 1960–2004.
8. Jung, J. H.; John, G.; Masuda, M.; Yoshida, K.; Shinkai, S.; Shimizu, T. *Langmuir* **2001**, *17*, 7229–7232.
9. Steed, J. W. *Chem. Commun.* **2011**, 1379–1383.
10. Liu, J. A.; Ma, J. T.; Chen, C. F. *Tetrahedron* **2011**, *67*, 85–91.
11. Sangeetha, N. M.; Maitra, U. *Chem. Soc. Rev.* **2005**, *34*, 821–836.
12. Hirst, A. R.; Escuder, B.; Miravet, J. F.; Smith, D. K. *Angew. Chem., Int. Ed.* **2008**, *47*, 8002–8018.
13. Allix, F.; Curcio, P.; Pham, Q. N.; Pickaert, G.; Jamart-Gregoire, B. *Langmuir* **2010**, *26*, 6818–16827.
14. Tritt-Goc, J.; Bielejewski, M.; Luboradzki, R.; Łapiński, A. *Langmuir* **2008**, *24*, 34–540.
15. Bielejewski, M.; Łapiński, A.; Luboradzki, R.; Tritt-Goc, J. *Langmuir* **2009**, *25*, 8274–8279.
16. Wilder, E. A.; Hall, C. K.; Khan, S. A.; Spontak, R. J. *Langmuir* **2003**, *19*, 6004–6013.
17. Pinault, T.; Isare, B.; Bouteiller, L. *ChemPhysChem* **2006**, *7*, 816–819.
18. Hanabusa, K.; Matsumoto, M.; Kimura, M.; Kakehi, A.; Shirai, H. *J. Colloid Interface Sci.* **2000**, *224*, 231–244.
19. Gronwald, O.; Shinkai, S. *J. Chem. Soc., Perkin Trans. 2* **2001**, 1933–1937.
20. Suzuki, A.; Yumoto, M.; Kimura, M.; Shirai, H.; Hanabusa, K. *Chem. Commun.* **2002**, 884–885.
21. Amanokura, N.; Kanekiyo, Y.; Shinkai, S.; Reinhoudt, D. N. *J. Chem. Soc., Perkin Trans. 2* **1999**, 1995–2000.
22. Jung, J. H.; Amaike, M.; Nakashima, S.; Shinkai, S. *J. Chem. Soc., Perkin Trans. 2* **2001**, 1938–1943.
23. Suzuki, M.; Nakajima, Y.; Sato, T.; Shirai, H.; Hanabusa, K. *Chem. Commun.* **2006**, 377–379.
24. Hirst, A. R.; Smith, D. K. *Langmuir* **2004**, *20*, 10851–10857.
25. Zhu, G.; Dordic, J. S. *Chem. Mater.* **2006**, *18*, 5988–5995.
26. Makarevic, J.; Jokic, M.; Peric, M.; Tomisic, V.; Kojic-Prodic, B.; Zinic, M. *Chem. –Eur. J.* **2001**, *7*, 3328–3341.
27. Edwards, W.; Lagadec, C. A.; Smith, D. K. *Soft Matter* **2011**, *7*, 110–117.
28. Bielejewski, M.; Tritt-Goc, J. *Langmuir* **2010**, *26*, 17459–17464.
29. Noack, F. *Prog. Nucl. Magn. Reson. Spectrosc.* **1986**, *18*, 171–276.
30. Kimmich, R.; Anoardo, E. *Prog. Nucl. Magn. Reson. Spectrosc.* **2004**, *44*, 257–320.
31. Steiner, E.; Yemloul, M.; Guendouz, L.; Leclerc, S.; Robert, A.; Canet, D. *Chem. Phys. Lett.* **2010**, *495*, 287–291.
32. Jeong, Y.; Friggeri, A.; Akiba, I.; Masunaga, H.; Sakurai, K.; Sakurai, S.; Okamoto, S.; Inoue, K.; Shinkai, S. *J. Colloid Interface Sci.* **2005**, *283*, 113–122.
33. Friggeri, A.; Gronwald, O.; van Bommel, K. J. V.; Shinkai, S.; Reinhoudt, D. N. *J. Am. Chem. Soc.* **2002**, *124*, 10754–10758.
34. Luboradzki, R.; Gronwald, O.; Ikeda, M.; Shinkai, S.; Reinhoudt, D. N. *Tetrahedron* **2000**, *56*, 9595–9599.
35. Gronwald, O.; Shinkai, S. *Chem.—Eur. J.* **2001**, *7*, 4328–4334.
36. Kowalczuk, J.; Jarosz, S.; Tritt-Goc, J. *Tetrahedron* **2009**, *65*, 9801–9806.
37. Bloembergen, N.; Purcell, E. M.; Pound, R. V. *Phys. Rev.* **1948**, *73*, 679–683.
38. Teng, C. L.; Hong, H.; Kihne, S.; Bryant, R. G. *J. Magn. Reson.* **2001**, *148*, 31–34.
39. Edzes, H. T.; Samulski, E. T. *J. Magn. Reson.* **1978**, *3*, 207–229.
40. Whaley, M.; Lawence, A. J.; Korb, J.; Bryant, R. G. *Solid State Nucl. Magn. Reson.* **1996**, *7*, 247–252.
41. Brownstein, K. R.; Tarr, C. E. *J. Magn. Reson.* **1977**, *26*, 17–24.
42. Bychuk, O. V.; O'Shaughnessy, B. J. *Chem. Phys.* **1994**, *101*, 772–780.
43. Stapf, S.; Kimmich, R. *Chem. Phys. Lett.* **1997**, *275*, 261–268.
44. Powels, J. G.; Neale, D. J. *Proc. Phys. Soc.* **1960**, *3*, 737–747.
45. Geen, D. K.; Powels, J. G. *Proc. Phys. Soc.* **1965**, *85*, 87–102.
46. Stapf, S.; Kimmich, R. *J. Chem. Phys.* **1995**, *103*, 2247–2250.
47. Negi, A. S.; Osuji, C. O. *J. Rheol.* **2010**, *54*, 943–958.
48. Yin, G.; Solomon, M. J. *J. Rheol.* **2008**, *52*, 785–800.
49. Manley, S.; Davidovitch, B.; Davies, N. R.; Cipelletti, L.; Bailey, A. E.; Christianson, R. J.; Gasser, U.; Prasad, V.; Segre, P. N.; Doherty, M. P.; Sankaran, S.; Jankovsky, A. L.; Shiley, B.; Bowen, J.; Eggers, J.; Kurta, C.; Lorik, T.; Weitz, D. A. *Phys. Rev. Lett.* **2005**, *95*, 048302–048306.
50. Schupper, N.; Rabin, Y.; Rosenbluh, M. *Macromolecules* **2008**, *41*, 3983–3994.